Biochemical and Biophysical Research Communications xxx (xxxx) xxx

Contents lists available at ScienceDirect

Biochemical and Biophysical Research Communications

journal homepage: www.elsevier.com/locate/ybbrc

Interaction of the chaperones alpha B-crystallin and CHIP with fibrillar alpha-synuclein: Effects on internalization by cells and identification of interacting interfaces

Maya Bendifallah, Virginie Redeker, Elodie Monsellier, Luc Bousset, Tracy Bellande, Ronald Melki*

CEA, Institut François Jacob (MIRcen) and CNRS, Laboratory of Neurodegenerative Diseases (U9199), 18 Route du Panorama, 92265, Fontenay-aux-Roses, France

ARTICLE INFO

Article history:
Received 29 March 2020
Accepted 17 April 2020
Available online xxx

Keywords:
Molecular chaperones
Protein-protein interactions
Protein-protein interfaces
Cross linking, mass spectrometry

ABSTRACT

The spread of fibrillar alpha-synuclein from affected to naïve neuronal cells is thought to contribute to the progression of synucleinopathies. The binding of fibrillar alpha-synuclein to the plasma membrane is key in this process. We and others previously showed that coating fibrillar alpha-synuclein by the molecular chaperone Hsc70 affects fibrils properties. Here we assessed the effect of the two molecular chaperones alpha B-crystallin and CHIP on alpha-synuclein fibrils uptake by Neuro-2a cells. We demonstrate that both chaperones diminish fibrils take up by cells. We identify through a cross-linking and mass spectrometry strategy the interaction interfaces between alpha-synuclein fibrils and alpha B-crystallin or CHIP. Our results open the way for designing chaperone-derived polypeptide binders that interfere with the propagation of pathogenic alpha-synuclein assemblies.

1. Introduction

Parkinson's disease and other synucleinopathies are associated with the aggregation of the protein alpha-synuclein (αSyn) into high molecular weight fibrillar aggregates [1,2]. Aggregated αSyn traffic between neuronal cells, seed the aggregation of endogenous monomeric αSyn and amplify [3–5]. This prion-like phenomenon is presumed to contribute to the stereotypic progression of synucleinopathies [5,6]. αSyn aggregates propagate through exosomes [7,8], tunneling nanotubes [9,10] and following their release to the extracellular space through export by living cells or liberation by dying cells [11–13]. The latter aggregates bind to the cell membrane and are internalized, primarily through endocytosis [14,15]. They eventually compromise the endo-lysosomal integrity [16] and reach the cytosol where they amplify by recruiting endogenous monomeric αSyn [17,18]. The resulting aggregates find next their way into naive, unaffected cells, perpetuating the cycle [17,19]. Fibrillar αSyn assemblies' formation and trafficking represent targets for therapeutic interventions [20]. Those assemblies bind to the cell membranes through numerous protein [21–25], and lipid [26,27] membrane partners, many of which are essential to cell physiology.

αSyn aggregates in the crowded cellular environment in the presence of a vast number of proteins, including molecular chaperones. Molecular chaperones, the first line of defense in protein homeostasis, interact with aggregating proteins [28,29]. Extensive research has reported that various chaperones, such as Hsp90, Hsp70, Hsp27 and alpha B-crystallin (αBc), interfere with the assembly of monomeric αSyn into fibrils [30,31,32,33,34,35]. Those molecular chaperones may bind aggregated αSyn *in vivo* as they have been shown to be present within αSyn-rich deposits within cells. This justifies characterizing thouroughly the interactions between molecular chaperones and αSyn [36,37,38,39,40,41], demonstrating chaperone binding to αSyn fibrils *in vitro*.

We previously demonstrated that Hsc70 binds fibrillar αSyn with high affinity [33,40]. Hsc70-coated αSyn fibrils are less toxic to cells compared to naked fibrils [33]. We further identified intermolecular surfaces of the interaction between Hsc70 and αSyn [39,40]. Here, we focused on human sHSP chaperone αBc and human C-terminus Hsc70-interacting protein (CHIP). αBc is one of the 2 subunits of the chaperone α-crystallin, a prominent component of the human eye lens that prevents aggregation of lens proteins,

* Corresponding author.
E-mail address: ronald.melki@cnrs.fr (R. Melki).

https://doi.org/10.1016/j.bbrc.2020.04.091

including itself. It consists of a mixture of oligomers ranging in size from 10 to 40 monomers [42]. αBc colocalizes with Lewy bodies in Parkinson's disease patients' neurons [43]. *In vitro*, αBc slows down the aggregation of many different proteins [30,44,34] and binds to preformed αSyn fibrils [37,41]. CHIP is a human dimeric chaperone of 34.8 kDa per monomer with E3 ubiquitin ligase activity [45]. It colocalizes with αSyn in Lewy bodies in Dementia with Lewy Body patient brains [46]. CHIP also targets αSyn oligomers for degradation and has a rescue effect in αSyn-induced-toxicity in different cellular models [46,47].

Here we assessed the uptake of αSyn fibrils assembled in the presence of αBc and CHIP by Neuro-2a cells. We demonstrate that both chaperones diminish αSyn fibrils take up by cells. Using an optimized cross-linking and mass spectrometry strategy, we identified the interaction interfaces between αSyn fibrils and αBc or CHIP. The two chaperones bind different αSyn polypeptides exposed at the surface of fibrils: a flexible segment located just before the fibrillar core for αBc and at a solvent accessible surface of the fibrillar core itself for CHIP. Our results may allow for the development of peptide ligands that can interfere with αSyn fibril prion-like propagation and subsequent disease progression.

2. Materials and methods

2.1. Cloning

A synthetic gene encoding αBc was purchased from GeneArt (Thermo Fisher Scientific). The vector allowing the bacterial expression of αBc was obtained by subcloning the corresponding synthetic gene into a pET14b vector (Novagen) at the NcoI-XhoI restriction sites. The pET151/D-TOPO vector (Invitrogen) allowing the bacterial expression of His_6, N-terminal-tagged CHIP with a V5 epitope was a gift from Jeffrey L. Brodsky. The His_6 tag is followed by a tobacco etch virus (TEV) protease cleavage site. Constructs were verified by DNA sequencing (Eurofins Genomics).

2.2. Expression & purification of recombinant proteins

Recombinant human wild-type α-Synuclein (αSyn) was expressed and purified as described [48].

Recombinant human wild-type αBc was expressed at 37 °C in *E.coli* strain BL21(DE3) (Stratagene) upon induction with IPTG (0.5 mM) for 3 h. Cells were harvested and resuspended in buffer A (50 mM Tris-HCl pH 8.5, 1 mM EDTA). After sonication and centrifugation, lysate supernatants were subjected to PEI precipitation (0.12% v/v). The supernatants were filtered and loaded onto a Q-sepharose FF column (GE Healthcare Lifesciences) equilibrated with buffer A, and eluted with buffer B (50 mM Tris-HCl pH 8.5, 1 mM EDTA, 100 mM NaCl). Fractions containing αBc were pooled and concentrated with a 3 kDa cutoff (Millipore), then loaded onto a size exclusion chromatography column (Superose 6 10/300 GL, GE Healthcare Lifesciences). αBc eluted with an apparent molecular weight corresponding to a multimer of 20–35 monomers. Gel filtration standards from Sigma-Aldrich (MWGF1000) were used for apparent molecular weight determination.

Recombinant His_6, N-terminal-tagged CHIP was expressed at 30 °C in *E.coli* strain BL21(DE3). Protein expression was induced by IPTG (0.5 mM) for 2 h. The cells were harvested and resuspended in buffer C (50 mM $NaPO_4$ pH 8.0, 300 mM NaCl, 3 mM β-mercaptoethanol [βME]). After sonication and centrifugation, lysate supernatants were filtered and loaded onto a 5 mL Talon metal affinity resin column (Clontech), equilibrated in buffer C. The protein was eluted in buffer C supplemented with 200 mM imidazole, then dialyzed in PBS. The His_6-tag was cleaved by addition of His_6-tagged tobacco etch virus (His-TEV) protease, produced using the plasmid pRK793 (Addgene), at a 1:20 His-TEV:chaperone molar ratio. 100% cleavage, as assessed by SDS-PAGE, was achieved upon incubating the mixtures for 1 h at 37 °C. The untagged proteins were purified by collecting the flow through of a 5 mL Talon metal affinity resin column.

After purification, all proteins were immediately filtered through sterile 0.22 μm filters, aliquoted and stored at −80 °C. The purity of all proteins was confirmed by SDS-PAGE and MALDI mass spectrometry (not shown). Protein concentrations were determined spectrophotometrically using the following extinction coefficients at 280 nm (M^{-1} cm^{-1}): 5960 for αSyn; 13,980 for αBc and 29,380 for CHIP.

2.3. Assembly of αSyn into fibrils and labeling

For kinetics and internalization experiments, monomeric αSyn was labeled by addition the aminoreactive fluorescent dye Alexa Fluor 488 (Alexa488, Invitrogen) using a protein:dye molar ratio of 10:1 based on initial monomer concentration. Labelling was performed following the manufacturer's recommendation. The reaction was quenched with Tris-HCl pH 7.5 (40 mM final concentration).

αSyn (100 μM monomer concentration) was incubated with increasing concentrations of αBc or CHIP (0–100 μM) in PBS at 37 °C under continuous shaking in an Eppendorf Thermomixer set at 600 rpm for 2 weeks. Aliquots were withdrawn at different time intervals from the assembly reactions and mixed with a primuline solution (10 μM). Primuline fluorescence was recorded with a Cary Eclipse spectrofuorimeter (Varian Medical Systems Inc) using excitation and emission wavelengths set at 400 and 480 nm, respectively. The nature of the fibrils obtained at the end of the aggregation reaction was assessed by transmission electron microscopy (TEM) as described below. The proportion of αSyn assembled into fibrils was assessed through a partition assay by centrifugation. To this aim, aliquots were withdrawn, subjected to centrifugation in an eppendorf 5415R centrifuge at 20,000 g and 20 °C, and the amount of protein in the supernatant and pellet fraction determined by SDS-PAGE analysis.

2.4. Transmission electron microscopy (TEM)

Fibrils were imaged by TEM in a Jeol 1400 transmission electron microscope (Jeol SAS) after adsorption onto carbon-coated 200 mesh grids and negative staining with 1% uranyl acetate. The images were recorded with a Gatan Orius CCD camera (Gatan Inc.).

2.5. Cell culture and internalization

Murine neuroblastoma Neuro-2a cells (ATCC) were cultured at 37 °C in humidified air with 5% CO2 in Dulbecco's modified Eagle's medium (DMEM, Sigma-Aldrich) containing 10% fetal bovine serum (Gibco, Thermo Fisher Scientific), 2 mM glutamine, 100 units.ml^{-1} penicillin (PAA Laboratories) and 100 μg ml^{-1} streptomycin (PAA Laboratories). All materials used for cell culture were from PAA Laboratories.

The internalization of Alexa488-labeled αSyn (1 μM equivalent monomer concentration) assembled in the presence or absence of αBc or CHIP was assessed. All fibrils were sonicated for 20 min in a VialTweeter powered by an ultrasonic processor UIS250v (250 W, 2.4 kHz; Hielscher Ultrasonic) set at 75% amplitude, 0.5 s pulses before dilution in DMEM. Neuro-2a cells cultured on 96-well plates were then incubated with these mixtures distributed in 5 independent wells. After 2 h, the medium was removed and Hoescht (Sigma-Aldrich), diluted at 0.2 μg/mL in serum-free, phenol red-free DMEM, was added for 30 min. The cells were washed twice

Please cite this article as: M. Bendifallah et al., Interaction of the chaperones alpha B-crystallin and CHIP with fibrillar alpha-synuclein: Effects on internalization by cells and identification of interacting interfaces, Biochemical and Biophysical Research Communications, https://doi.org/10.1016/j.bbrc.2020.04.091

and 0.1% Trypan Blue (Sigma-Aldrich) was added to quench the fluorescence of Alexa488-labeled αSyn fibrils that were plasma membrane-bound. For each well, Alexa488 and Hoechst fluorescences were recorded on a Clariostar microplate reader (BMG LABTECH). For each condition, the Alexa488 fluorescence value was considered and averaged over the 5 wells only if the Hoescht value was not significantly different from the one of untreated cells. Three independent experiments were conducted.

2.6. Chemical cross-linking and western blotting

Cross-linking experiments of chaperones with fibrillar αSyn were performed in PBS using αSyn alone (100 μM), chaperones alone (either 50 μM for αBc, or 33 μM for CHIP), or αSyn (100 μM) assembled into fibrils in the presence of chaperones (either 50 μM of αBc, corresponding to an αSyn:αBc molar ratio of 2:1; or 33 μM of CHIP, corresponding to an αSyn:CHIP molar ratio of 3:1) as described above. After two weeks of assembly, fibrillar αSyn samples were centrifuged at 100,000 g in a TL100 tabletop ultracentrifuge (Hitachi) for 30 min at 20 °C. The pellets were allowed to swell in PBS overnight before gentle resuspension. The final concentrations of αSyn fibrillar material and chaperones in the pellets were assessed by a partition assay by ultracentrifugation as described above.

The samples were exposed to various crosslinkers: glutaraldehyde (GA, ~5 Å spacer arm for monomeric glutaraldehyde, Sigma-Aldrich); bis(sulfosuccinimidyl) glutarate (BS2G, 7.7 Å spacer arm, Pierce); bis(sulfosuccinimidyl) suberate (BS^3, 11.4 Å spacer arm, Pierce); 3,30-dithiobis(sulfosuccinimidylpropionate) (DTSSP, 12 Å spacer arm, Pierce); or N-(3-dimethylaminopropyl)-N′-ethylcarbodiimide hydrochloride (EDC) with N-hydroxysulfosuccinimide (Sulfo-NHS) (0 Å spacer arm, Thermo Fisher Scientific) at a 1:1.25 EDC:Sulfo-NHS molar ratio. For GA, BS2G, BS^3 and DTSSP, reactions were quenched with the addition of Tris-HCl pH 7.5 (50 mM final concentration). For EDC/Sulfo-NHS, reactions were quenched with the addition of βME (20 mM final concentration) and Tris-HCl pH 8.2 (50 mM final concentration).

A specific αSyn-αBc cross-linked complex was obtained with GA exposition for 30 min at RT using a total protein:GA molar ratio of 1:1, corresponding to the following GA concentrations: 32 μM for αBc alone; 88 μM for αSyn fibrils alone; and 100 μM for αSyn fibrils formed in the presence of αBc. Total protein:GA molar ratios of 1:2 and 1:5, corresponding to 77/82/100 μM and 192/408/500 μM GA, led to the formation of higher order intermolecular cross-links among chaperones and fibrils alone.

A specific αSyn-CHIP cross-linked complex was obtained with EDC/Sulfo-NHS exposition for 30 min at RT using a total protein:EDC:Sulfo-NHS molar ratio of 1:10:12.5, corresponding to the following EDC/Sulfo-NHS concentrations: 320/400 μM for CHIP alone; 823/1029 μM for αSyn fibrils alone; 1178/1473 μM for αSyn fibrils formed in the presence of CHIP. Total protein: EDC:Sulfo-NHS molar ratio of 1:20:25 or at fixed concentrations of 2945/3683 μM corresponding to total protein:EDC:Sulfo-NHS molar ratios of 1:91:115, 1:36:45 and 1:25:31, respectively, led to the formation of higher order intermolecular cross-links among chaperones and fibrils alone.

In order to solubilize protein samples before SDS-PAGE analysis, all samples were first vacuum-dried then dissociated by addition of 10–20 μl of pure hexafluoroisopropanol (HFIP, Sigma-Aldrich). After incubation for 1 h in HFIP at RT, samples were evaporated before resuspension in denaturing Laemmli buffer, with the exception of DTSSP cross-linked samples which were resuspended in the same buffer without βME. Samples were heated for 5 min at 80 °C and loaded onto 7.5% tris-tricine gels.

For Western blot analysis, proteins separated by SDS-PAGE were transferred to nitrocellulose membranes (GE Healthcare). The membranes were first analyzed using an anti-αSyn antibody, stripped, and then revealed with an anti-αBc or anti-CHIP antibody. Briefly, the membranes were blocked in 3% skim milk in TBS-Tween 0.5%, probed with a primary then secondary antibody and developed with the enzyme-coupled luminescence technique (ECL, Thermo Fisher Scientific) using a ChemiDoc™ MP Imaging System (BioRad). The primary and secondary antibodies combinations used were the following: SYN1 antibody (1/5000, 610,787 BD Biosciences) followed by anti-mouse-HRP (1/5000, GTX 213111-01 Genetex) for αSyn detection, and rabbit polyclonal antibodies (1/5000) we raised against αBc or CHIP followed by anti-rabbit-HRP (1/5000, A120–101P Bethyl). For polyclonal antibody immunopurification, 1–10 mg of purified antigen protein was separated into a 15% SDS-PAGE gel and further transferred to a nitrocellulose membrane (GE Healthcare). The antigen-containing membrane was pre-incubated with 100 mM glycine pH 2.5 for 10 min before being blocked with 5% skim milk in TBS-Tween 0.05% and further incubated overnight in the anti-αBc or anti-CHIP antibody-containing serum. Polyclonal antibodies against αBc or CHIP were eluted with 2 mL 100 mM glycine pH 2.5 for 2 min. After immediate neutralization with addition of Tris-HCl pH 8.5, the immunopurified antibodies were dialyzed into PBS pH 7.4, 30% glycerol. Stripping of the membrane between two immunodetections was achieved with 100 mM βME, 62.5 mM Tris-HCl pH 6.8, 2% SDS for 1 h at 50 °C.

2.7. Peptide preparation and NanoLC-MS/MS identification of cross-linked peptides

Bands of interest were excised and cut in pieces of about 2 mm^2. Each band was subjected to washing and in-gel tryptic digestion as described [49], without reduction and alkylation. Tryptic digestion was performed overnight at 37 °C using Trypsin Gold (Promega) at a concentration of 10 ng/μl in 25 mM ammonium bicarbonate. Tryptic peptides were extracted using two volumes of 60% acetonitrile (ACN), 0.1% formic acid for 1 h. The supernatant was recovered and a second extraction was performed by addition of one volume of 100% ACN for 30 min. The two supernatants of extracted peptides were pooled and vacuum dried. Tryptic peptides were resuspended in 0.1% formic acid (v/v) prior to nanoLC-MS/MS analysis.

Tryptic peptides were analyzed with a Data Dependent acquisition method by selecting the 20 most intense precursors for CID fragmentation using a Triple-TOF 4600 mass spectrometer (ABSciex) coupled to a nanoRSLC ultra performance liquid chromatography (UPLC) system (Dionex, Thermo Fisher Scientific) as previously described [50] with the following exceptions. The analytical column was an Acclaim PepMap RSLC C18 (75 μm i.d. × 50 cm, 2 μm, 100 Å, Thermo Fisher Scientific). Peptides were loaded at 6 μl/min and separated with a gradient of 5–35% 0.1% formic acid in 100% ACN.

2.8. NanoLC-MS/MS data analysis

NanoLC-MS/MS raw data were converted into mgf data files using the MS Data Converter software (Peakview, ABSciex). Sequence coverage of the proteins was determined through database searching using the Mascot search engine (Matrix Science; version 2.6) with the SwissProt mammalian database (SwissProt_2018_10 database release) together with a decoy database search. Only peptides with a mascot score above 20 were considered. Inter-molecular cross-linked peptides between αSyn and

Please cite this article as: M. Bendifallah et al., Interaction of the chaperones alpha B-crystallin and CHIP with fibrillar alpha-synuclein: Effects on internalization by cells and identification of interacting interfaces, Biochemical and Biophysical Research Communications, https://doi.org/10.1016/j.bbrc.2020.04.091

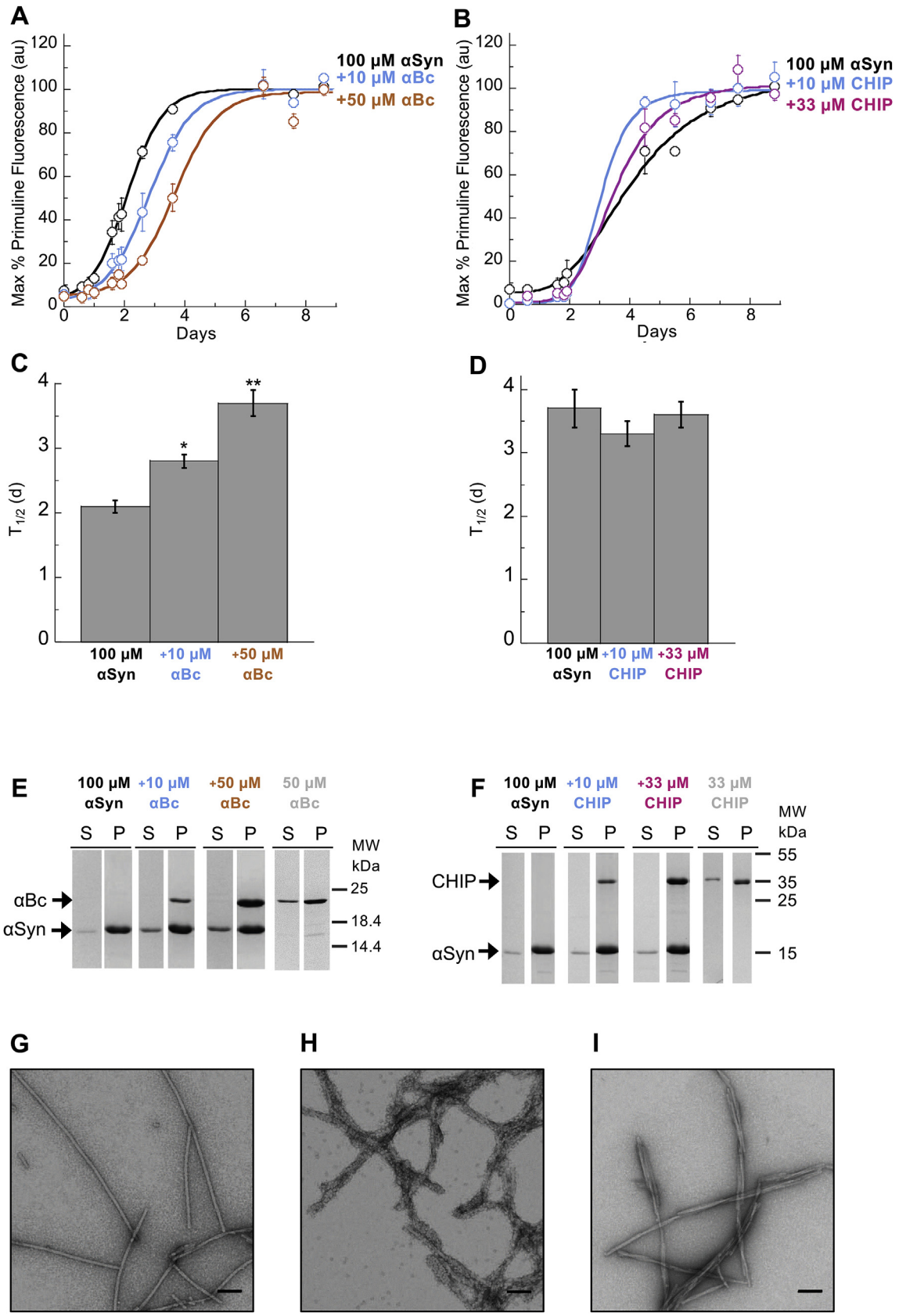

Fig. 1. αSyn fibrillation in presence of chaperones. (A–B) Time-course fibrillation of αSyn-Alexa488 (100 µM) in the presence of increasing concentrations of αBc (A) or CHIP (B) was followed by primuline fluorescence. Chaperone concentrations of 0 µM, 10 µM, 20 µM, 33 µM, 50 µM are represented as αSyn:chaperone molar ratios of 1:0 (black), 10:1 (blue), 3:1 (pink) or 2:1 (orange) respectively. Means and their associated standard error values were calculated from three independent experiments. Lines through the data points are the best sigmoidal fit. **(C–D)** Half-time ($t_{1/2}$) of αSyn-Alexa488 aggregation in the presence of increasing concentrations of αBc (C) or CHIP (D). For each independent experiment, the $t_{1/2}$

Please cite this article as: M. Bendifallah et al., Interaction of the chaperones alpha B-crystallin and CHIP with fibrillar alpha-synuclein: Effects on internalization by cells and identification of interacting interfaces, Biochemical and Biophysical Research Communications, https://doi.org/10.1016/j.bbrc.2020.04.091

chaperones were searched using the STAVROX software (version 3.6.6.6), [51]. For GA, which exists as a mixture of monomers (free aldehyde or cyclic hemiacetal forms) or different polymers [52], we set the mass modification to 64.031 or 82.042 to search for interprotein peptides cross-linked by a free aldehyde or a cyclic hemiacetal GA, respectively, on a list of potentially reactive amino acids for sites 1 and 2 as reported in the literature, or as indicated by their physico-chemical properties (Lysine, Serine, Threonine, Tyrosine, Arginine, Tryptophan, Phenylalanine, Proline, and N-terminus). One interprotein cross-link by a cyclic hemiacetal monomer of GA was identified and confirmed. For EDC, mass modification was set to 18.01 Da for interprotein cross-linked peptides modified on Lysine, Serine, Threonine, Tyrosine, and N-terminus for site 1 and Aspartate, Glutamate and C-terminus for site 2. For both Mascot and Stavrox searches, the parent and fragment ion mass tolerances were 25 ppm and 0.05 Da, respectively, oxidation of methionine was set as a variable modification, and trypsin cleavage was semi-specific. Candidate cross-linked peptides were validated after confirmation of their absence in the control samples and manual analysis of their MS/MS spectra.

3. Results

Extensive studies have reported that chaperones interact with amyloid-forming proteins and are thus good candidates to prevent either the aggregation reaction or the interaction of the resulting amyloids with binding partners within the cytosol or at the plasma membrane. Previous work in our laboratory showed that the molecular chaperone Hsc70 reduces αSyn assembly and affects preformed fibrils binding and subsequent toxicity [33].

We wanted to assess if the ability to bind preformed αSyn fibrils is a generic property of molecular chaperones, in the perspective of expanding our arsenal of chaperones able to modify αSyn fibril surfaces and interfere with their cell-to-cell propagation. We selected two different molecular chaperones that we considered promising based on previous data demonstrating their association or colocalization with aggregated αSyn, either *in vitro* or in pathological lesions or inclusions observed in the brains of patients with synucleinopathies [43,37,34,46,47,41]: the human sHSP chaperone αB-crystallin (αBc) and human C-terminus Hsc70-interacting protein (CHIP).

Effect of αBc and CHIP on αSyn fibrils take-up by Neuro-2a cells.

We first assessed the effect of αBc and CHIP on the assembly of αSyn into fibrils at different αSyn:molecular chaperone molar ratios (Fig. 1). We used Alexa488-labeled monomeric αSyn for these assembly reactions, in order to obtain labeled αSyn fibrils in complex with unlabeled chaperones and assess the uptake of the resulting fibrils by Neuro-2a cells. The kinetics of aggregation were followed by primuline fluorescence. Notably, the assembly kinetics of unlabeled and Alexa488-labeled αSyn into fibrils, as well as the fibrils abilities to seed, are comparable [53].

Fibrillation kinetics of αSyn in presence of increasing concentrations of αBc show that αBc significantly slows down αSyn aggregation, starting from an αSyn:αBc molar ratio of 10:1 (Fig. 1A, C). At a 2:1 αSyn:αBc molar ratio, αBc did not significantly modify neither the amount (Fig. 1E) nor the morphology (Fig. 1H) of fibrillar αSyn. While CHIP had no significant effect neither on αSyn kinetics of aggregation (Fig. 1B,D) nor on the amount (Fig. 1F) of aggregated αSyn, it had an effect on the morphology of fibrils. They appeared more twisted than those formed without molecular chaperones (Fig. 1I). Increases of αBc or CHIP concentrations induced an increase of the amount of chaperones bound to αSyn fibrils, as identified thorugh a sedimentation assay (Fig. 1E and F).

We next assessed the internalization of αSyn fibrils formed in the presence of αBc or CHIP by Neuro-2a cells (Fig. 2A and B, respectively). Neuro-2a cells, in 96-well plates, were exposed for 2 h to Alexa488-labeled αSyn fibrils (1 μM) pre-incubated or not with αBc or CHIP (0, 2 and 10 μM), prior to Trypan blue addition and quantification of Alexa488 fluorescence in a plate-reader. αSyn fibril fluorescence quenching by Trypan blue allowed us to determine accurately the amount of internalized fibrils in a dose-dependent manner. We used Hoescht staining to ascertain that the number of cells remained constant (see Material & Methods). As a positive control for this experiment, we examined the effect of heparin, a ligand of cell membrane heparan sulfate proteoglycans that have been implicated in αSyn internalization [24]. When preformed αSyn-Alexa488 fibrils were pre-incubated with 0.2 μg/mL heparin, we observed an 83% reduction of their internalization (Fig. S1), in agreement with previous reports [24]. αSyn-Alexa488 fibrils assembled in presence of increasing amounts of αBc or CHIP take-up by Neuro-2a cells decreased in a chaperone concentration-dependent manner (Fig. 2). We conclude from these experiments that αBc or CHIP affect fibrillar αSyn uptake by Neuro-2a cells, most probably by binding the fibrils and changing their surface properties.

Identification of interaction surfaces between fibrillar αSyn, αBc and CHIP through chemical cross-linking.

We next mapped the surface interfaces between αBc or CHIP and fibrillar αSyn to further characterize the interactions. We used chemical cross-linking and mass spectrometric identification of cross-linked peptides to this aim [54,39,55,40].

αSyn fibrils (100 μM) formed in presence or absence of αBc (50 μM) or CHIP (33 μM) were exposed to different cross-linkers at different total protein to crosslinker molar ratios. αSyn fibrils, αBc and CHIP were exposed individually to the cross-linkers in control reactions. The cross-linkers we used had distinct structural-chemical characteristics. Three homobifunctional water soluble NHS-ester cross-linkers specific to nucleophilic groups (predominantly primary amines e.g. proteins N-terminus and Lysine residues, but also Tyrosine, Serine and Threonine) with varying spacer arm lengths: 7.7, 11.4 and 12 Å for BS2G, BS^3 and DTSSP, respectively, were used. We further used the heterobifunctional zero length carbodiimide crosslinker EDC that crosslinks primary amines to carboxyl groups (e.g. Glu, Asp and proteins C-terminus) in the presence of Sulfo-NHS. Finally, we also used GA, known for its efficiency, but also its limited specificity and molecular heterogeneity with a ~5 Å spacer arm for the monomer [52]. The cross-linking reactions products were analyzed by SDS-PAGE to identify fibrillar αSyn-αBc or fibrillar αSyn-CHIP complexes, observed neither in the fibrillar αSyn nor in the chaperone control samples subjected to identical cross-linking conditions. The total protein to cross-linker ratio was optimized. A 1:1 and 1:10:12.5 total protein to cross-linker ratios were selected for fibrillar αSyn-αBc cross-linking with GA and for fibrillar αSyn-CHIP cross-linking with EDC/Sulfo-NHS, respectively. Finally, as the reaction involved cross-

parameter was extracted from the best fit to a sigmoid function. The means are their associated standard error values were calculated from three independent experiments. Statistical significance was determined through an unpaired student's t-test with equal variance. Annotations indicating level of significance are as follows: *p < 0.05; **p < 0.01. Legends state αSyn:chaperone molar ratios. **(E–F)** Supernatant and pellet samples at the end of the aggregation reactions in absence or presence of αBc (E) or CHIP (F) resolved by SDS-PAGE and coomassie blue staining. Legends state αSyn and chaperone concentrations. **(G–I)** TEM micrographs of αSyn-Alexa488 fibrils formed alone (G), fibrils formed in presence of αBc (2:1 αSyn:αBc molar ratio, H), and fibrils formed in presence of CHIP (3:1 αSyn:CHIP molar ratio, I). (For interpretation of the references to colour in this figure legend, the reader is referred to the Web version of this article.)

Please cite this article as: M. Bendifallah et al., Interaction of the chaperones alpha B-crystallin and CHIP with fibrillar alpha-synuclein: Effects on internalization by cells and identification of interacting interfaces, Biochemical and Biophysical Research Communications, https://doi.org/10.1016/j.bbrc.2020.04.091

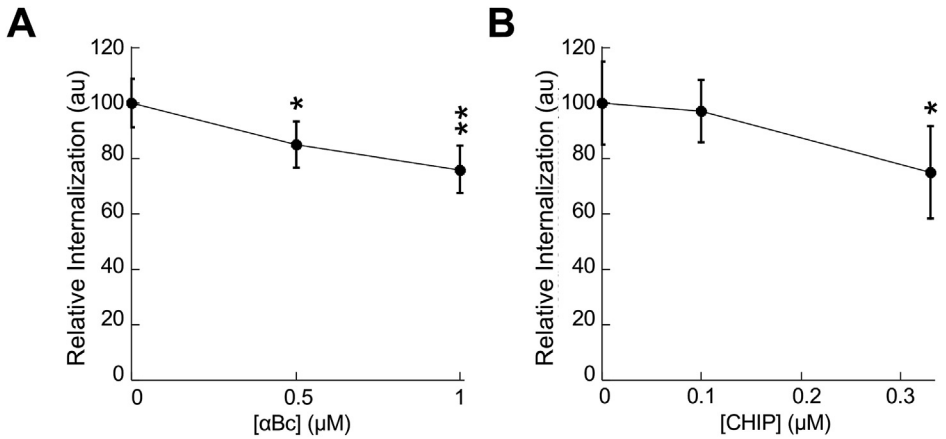

Fig. 2. Effect of αBc and CHIP on αSyn fibril uptake by Neuro-2a cells. αSyn-Alexa488 fibrils were assembled at 100 μM in the absence or in the presence of 50 or 100 μM αBc or 10 or 33 μM CHIP. After two weeks of fibril formation, the mixture was diluted 100x in DMEM and incubated for 30 min at 37 °C. Neuro-2a cells in 96-well plates were exposed for 2 h to αSyn-Alexa488 fibrils assembled in the presence of αBc (A) or CHIP (B). Trypan blue was added after extensive washing to quench the fluorescence of plasma membrane-bound αSyn-Alexa488 fibrils. The amount of internalized αSyn-Alexa488 was measured on a fluorescence plate reader. Means and their associated standard deviation values are calculated over 5 wells. In each case we performed three independent experiments; one representative experiment is shown. The results and the associated significances are reported to the internalization in the absence of chaperone. Statistical significance was determined through an unpaired student's t-test with equal variance. Annotations indicating level of significance are as follows: *p < 0.05; **p < 0.01; ***p < 0.001.

linking fibrillar αSyn to the molecular chaperones, the cross-linked high molecular weight complexes were dissociated to allow their analysis by SDS-PAGE.

Specific cross-linked complexes were observed with GA and fibrillar αSyn with αBc (Fig. 3A) upon staining the polyacrylamide gel with Coomassie blue and on western blots using antibodies directed against αSyn and αBc. The exposure of αSyn fibrils alone to GA yielded protein bands representing monomers, dimers, trimers and tetramers, while that of αBc alone did not affect the intensity of the dimeric form of the protein. Higher concentrations of GA led to the formation of cross-linked higher molecular weight αSyn and αBc species (Fig. S2A). When αSyn-αBc complex was cross-linked with GA, a unique and specific protein band appears at around 40 kDa (arrow). Western blot analyses with antibodies directed against αSyn and αBc confirms that this specific band contains both proteins and thus corresponds to a covalent αSyn-αBc complex. Its apparent molecular mass of 40 kDa suggests it is formed of one αSyn and one αBc monomer. The band of interest corresponding to the αSyn-αBc complex was thus cut off the gel and subjected to trypsin digestion. The resulting peptides were analyzed by nano-liquid chromatography coupled to tandem mass spectrometry (nanoLC-MS/MS). For the αSyn-αBc complex, using database searching as described in Materials & Methods, we obtained a sequence coverage of 100% for αSyn and 97% for αBc. Using the Stavrox software [51], we identified one αSyn-αBc inter-protein cross-linked peptide that was absent from control bands (monomeric or dimeric αSyn or αBc with or without GA cross-linking) and was validated manually. This peptide was identified as a quadruple peptide ion with a mass-to-charge of 622.847, consistent with an inter-peptide cross-link that covalently binds two peptide sequences and thus is highly charged (Fig. 3B). Its fragmentation spectrum, presented in Fig. 3B, identified the cross-linked peptides and sites. The y and b fragments ions series reported in Fig. 3C identified the αSyn [33–43] and αBc [153–163] sequences of the cross-linked peptide with a cross-link between Lys-34 from αSyn and Thr-162 from αBc. The mass deviation of −3.02 ppm measured between the experimental and the theoretical mass of this cross-linked peptide further validated the identification. Interestingly the αBc peptide [153–163] in which Thr-162 is cross-linked is located in the flexible, unstructured C-terminus of the chaperone [44], and the αSyn peptide [33–43] in which Lys-34 is cross-linked to αBc is exposed to the solvent in the fibrillar structures of αSyn (PBD code 6rt0 and 6rtb) we recently solved (Fig. 3E), [56].

Fibrillar- αSyn-CHIP cross-links obtained using EDC/Sulfo-NHS were resolved by SDS-PAGE and detected both by coomassie blue staining and Western blot using antibodies against αSyn and CHIP (Fig. 4A). A dimeric for of CHIP was observed upon treatment of the protein with EDC/Sulfo-NHS, confirming its dimeric state. Higher concentrations of EDC/Sulfo-NHS led to the formation of cross-linked higher molecular weight αSyn and CHIP (Fig. S2B). When αSyn-CHIP complex was cross-linked with EDC, a unique and specific protein band appears at an apparent molecular mass around 55 kDa (arrow). Western blot analyses with antibodies directed against αSyn and CHIP confirm that this specific additional band contains both proteins and thus corresponds to a covalent αSyn-CHIP complex. Its apparent molecular mass of about 55 kDa suggests it is constituted by one αSyn and one CHIP monomer. The band of interest corresponding to the αSyn-CHIP covalent complex was cut off the gel and in-gel digested using trypsin and the resulting peptides were further analyzed by nanoLC-MS/MS as described above. By database search as described in Material and Methods, we obtained a sequence coverage of 100% for αSyn and 85% for CHIP. Using the Stavrox software [51], we identified one αSyn-CHIP inter-protein cross-linked peptide that was absent from control bands (monomeric or dimeric αSyn or CHIP with or without EDC cross-linking) and was validated manually. This peptide was identified as a quadruple charged ion with a mass-to-charge of 616.136 (Fig. 4B). Its fragmentation spectrum presented in Fig. 4B unambiguously identified the cross-linked peptides and sites. The y and β fragments ions, reported in Fig. 4C, identified the αSyn [61–80] and CHIP [254–262] sequences of the cross-linked peptide with a cross-link between Glu-61 from αSyn and Lys-254 from CHIP. Finally, the mass deviation of 4.17 ppm measured between the experimental and the theoretical mass of this cross-linked peptide further validated the identification. Interestingly, CHIP peptide [254–262], in which Lys-254 (in purple, space fill, Fig. 4D) has been cross-linked to fibrillar αSyn, is located within the CHIP U-box domain [45] while αSyn peptide [61–80], in which Glu61 (red sphere, Fig. 4E) was cross-linked to CHIP, is located in the non-amyloid component (NAC) region and is accessible to the solvent in the fibrillar structures of αSyn (PBD code 6rt0 and 6rtb) we recently solved [56].

Please cite this article as: M. Bendifallah et al., Interaction of the chaperones alpha B-crystallin and CHIP with fibrillar alpha-synuclein: Effects on internalization by cells and identification of interacting interfaces, Biochemical and Biophysical Research Communications, https://doi.org/10.1016/j.bbrc.2020.04.091

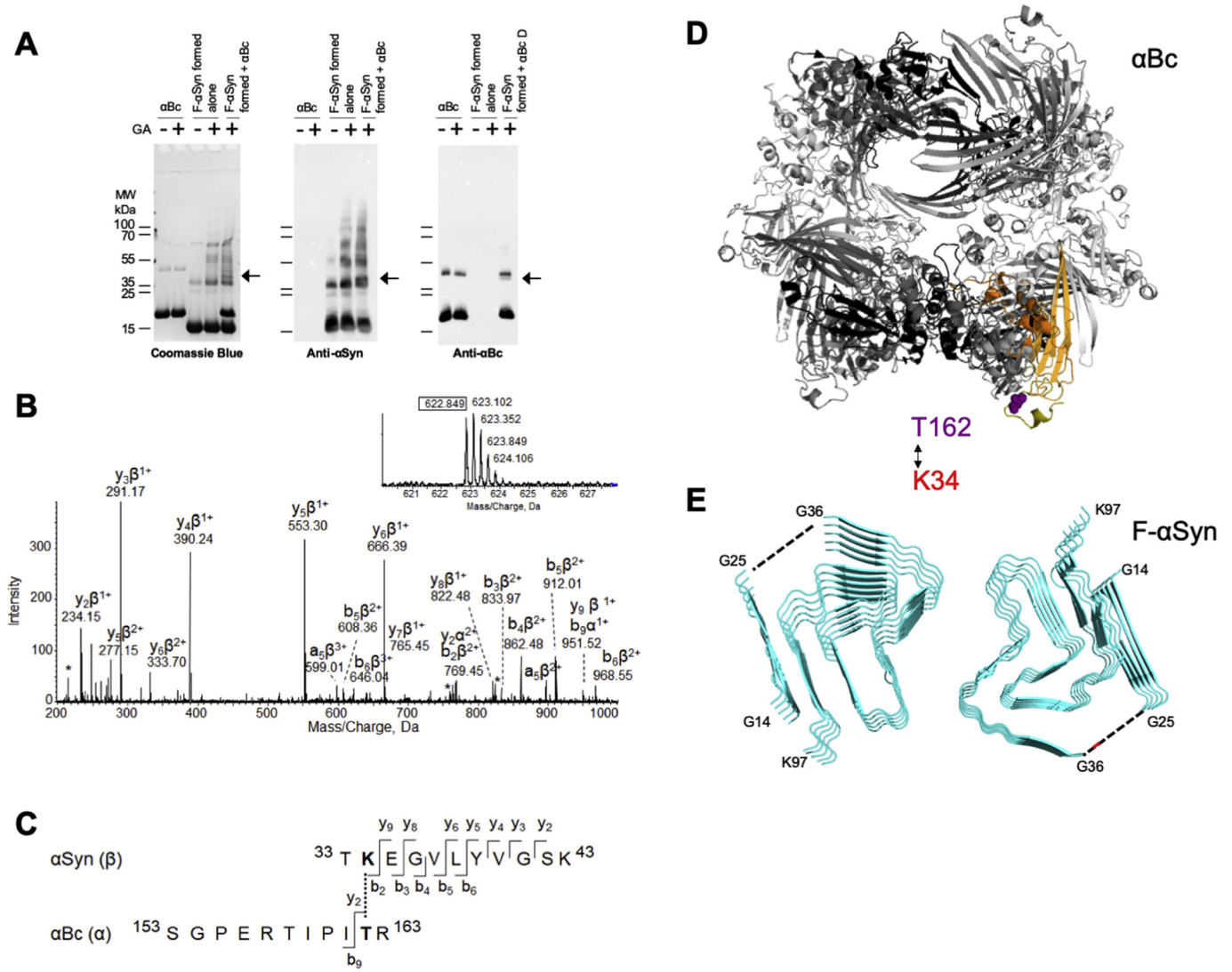

Fig. 3. Cross-linking of αBc to αSyn fibrils by glutaraldehyde. (**A**) Cross-linking reaction protein products were separated on a 7.5% tris-tricine SDS-PAGE and detected by coomassie blue staining and immunodetection by Western blot using detections with either SYN1 anti-αSyn or in-house-immunopurified rabbit polyclonal anti-αBc antibodies. αBc alone, αSyn fibrils (F-αSyn) alone or αSyn fibrils formed in the presence of αBc (2:1 αSyn:αBc molar ratio) were exposed to the glutaraldehyde (GA) cross-linker at the same total protein:GA molar ratio (1:1). The arrows show the band of the αSyn-αBc complex of interest. **(B–C)** NanoLC-MSMS analysis and data analysis using the Stavrox software identified the peptide [153–163] from αBc cross-linked with peptide [33–43] from αSyn fibrils. In B, the fragmentation spectrum of the quadruple-charged cross-linked precursor ion at the monoisotopic *m*/*z* 622.847 (on the top) is annotated with the identified fragments and their charge state. Loss of water (asterisks) and internal fragments (i) are indicated. In C, the identified fragments are indicated on the cross-linked sequences. The α and β sequences correspond to the αBc [153–163] and αSyn [33–43] peptides, respectively. The identified cross-link involves residues Thr-162 and Lys-34 from αBc and αSyn, respectively. **(D)** Location of the cross-linked threonine in a model structure of an αBc 24-mer (PDB accession number 2ygd, 9.4 Å resolution). Thr-162 (T162) is represented by a purple sphere. (**E**) Location of the cross-linked lysine in αSyn fibrils (PDB accession number 6rt0). Lys-34 (K34) is in a flexible portion of the sequence, not resolved by cryo-EM, and sketched by a dotted black line; K34 itself is represented by a red line. Figures D–E were generated with PYMOL (http://www.pymol.org). . (For interpretation of the references to colour in this figure legend, the reader is referred to the Web version of this article.)

4. Discussion

The aggregation of distinct proteins is hallmark of neurodegenerative disease [29]. Molecular chaperones interfere with this process and/or are a component of the resulting aggregates [29,34,43,44,46,57,58]. αSyn fibrillar aggregates are capable of propagating between neuronal cells and consequently contribute to disease progression in synucleinopathies [3,4]. Therefore, identifying the contribution of molecular chaperones within this process and determining whether they bind αSyn fibrils and affect their propagation is of particular interest. It has been previously shown that Hsc70 not only reduces aggregation of αSyn [33] into fibrils, but also binds the fibrils and affects their toxicity [33]. Furthermore, we identified inter-molecular interaction surfaces between Hsc70 and αSyn using covalent cross-linking and mass spectrometry [39,40].

The binding of molecular chaperones to preformed αSyn fibrils have been assessed on rare occasions [36,37,38,41]. The molecular chaperone αBc, we used here, was shown for instance to bind to preformed αSyn fibrils [37,41]. We thus went further and assessed the take-up by cultured cells of neuronal origin of fibrillar αSyn assembled in the presence of molecular chaperones. We show that the molecular chaperones αBc and CHIP bind efficiently to αSyn fibrils generated in their presence and affect their take-up by Neuro-2a cells. We further identified the inter-molecular interaction interfaces between fibrillar αSyn and αBc or CHIP.

αBc binds to fibrillar αSyn through its C-terminal unstructured domain. Our cross-linking studies show that αBc interacts with

Please cite this article as: M. Bendifallah et al., Interaction of the chaperones alpha B-crystallin and CHIP with fibrillar alpha-synuclein: Effects on internalization by cells and identification of interacting interfaces, Biochemical and Biophysical Research Communications, https://doi.org/10.1016/j.bbrc.2020.04.091

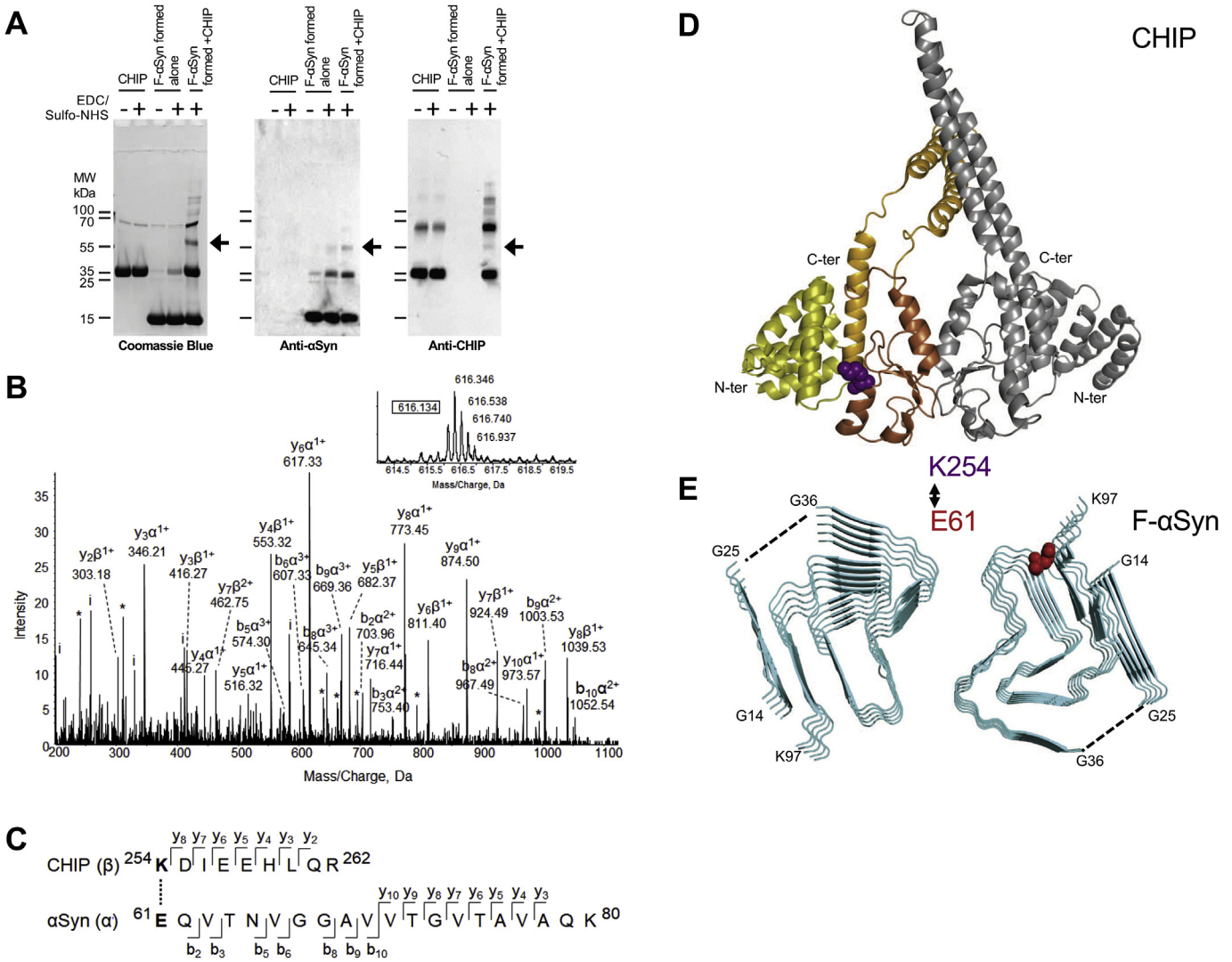

Fig. 4. Cross-linking of CHIP to αSyn fibrils by EDC/SulfoNHS-ester. **(A)** Cross-linking reaction protein products were separated on a 7.5% tris-tricine SDS-PAGE and detected by coomassie blue staining and immunodetection by Western blot using detections with either SYN1 anti-αSyn or in-house-immunopurified rabbit polyclonal anti-CHIP antibodies. CHIP alone, αSyn fibrils alone or αSyn fibrils formed in the presence of CHIP (3:1 αSyn:CHIP molar ratio) were exposed with EDC/SulfoNHS-ester cross-linker at same total protein:EDC:Sulfo-NHS molar ratio (1:10:12.5). The arrows show the band of the αSyn-CHIP complex of interest. **(B–C)** NanoLC-MSMS analysis and data analysis using the Stavrox software identified the peptide [254–262] from CHIP cross-linked with peptide [61–80] from αSyn fibrils. In B, the fragmentation spectrum of the quintuple-charged cross-linked precursor ion at the monoisotopic *m/z* 616.136 (on the top) is annotated with the identified fragments and their charge state. Loss of water (asterisks) and internal fragments (i) are indicated. In C, the identified fragments are indicated on the cross-linked sequences. The α and β sequences correspond to the αSyn [61–80] and CHIP [254–262] peptides, respectively. The cross-link involves residues Lys-254 and Glu-61 from CHIP and fibrillary αSyn, respectively. **(D)** Location of the cross-linked lysine in a CHIP dimer (Protein Data Bank accession number 2C2L, of murine CHIP, sharing 98% sequence identity with human CHIP). Lys-254 (K254) is represented by a purple sphere. The helical hairpin domains are in light orange, the tetratricopeptide repeat (TPR) domains are in yellow; the U-box domains are in bright orange. (**E**) Location of the cross-linked glutamate in αSyn fibrils (PDB accession number 6rt0). Glu-61 (E61) is represented by a red sphere. Figures D–E were generated with PYMOL (http://www.pymol.org).. (For interpretation of the references to colour in this figure legend, the reader is referred to the Web version of this article.)

αSyn fibrils. A unique intermolecular peptide was identified, where Thr-162 from αBc and Lys-34 from αSyn fibrils were cross-linked by GA. Lys-34 from αSyn is located within a flexible loop exposed to the solvent and αSyn fibril binders in the αSyn fibrillar structures (PBD code 6rt0 and 6rtb) we recently solved (Fig. 3E), [56]. Thr-162 from αBc lies in the unstructured C-terminal domain of αBc (Fig. 3D). αBc has been shown to interact with monomeric αSyn through a different region, namely a conserved β4/β8 surface lying within its core [59]. Indeed, αBc-core prevents the aggregation of αSyn [37,60]. Another heat shock protein, Hsp27, prevents the aggregation of αSyn and binds αSyn fibrils [37,61]. Interestingly, and in contrast with the whole protein, truncated Hsp27 containing only the conserved β4/β8 α-crystallin core domain loses its ability to bind αSyn fibrils [61]. Furthermore, dimeric, untruncated mutant Hsp27 binds αSyn fibrils, suggesting that residues outside of the core region of the conserved α-crystallin domain play a role in αSyn fibril binding [61].

CHIP binds to fibrillar αSyn through its C-terminal U-box domain. As for αBc, we mapped the interfaces between αSyn fibrils and the molecular chaperone CHIP. One inter-molecular peptide was identified, where Lys-254 from CHIP and Glu-61 from αSyn fibrils were cross-linked by EDC. Glu-61 from αSyn is located at one tip of the αSyn non-amyloid component (NAC) region and is exposed to the solvent (Fig. 4E), [56]. Lys-254 from CHIP is located in the C-terminal U-box domain of the chaperone (Fig. 4D), responsible for CHIP binding to ubiquitin-conjugating enzymes [45]. This result is

Please cite this article as: M. Bendifallah et al., Interaction of the chaperones alpha B-crystallin and CHIP with fibrillar alpha-synuclein: Effects on internalization by cells and identification of interacting interfaces, Biochemical and Biophysical Research Communications, https://doi.org/10.1016/j.bbrc.2020.04.091

coherent with previously published data. Indeed, a CHIP variant devoid of the Hsp70-binding N-terminal tetratricopeptide repeat domain (TPR, in yellow in Fig. 4D) but in which the U-box domain was still present, was able to immunoprecipitate αSyn [47].

It is worth noting that the interaction areas we identified within the αBc-αSyn fibril or CHIP-αSyn fibril complexes are not exhaustive as the cross-linking and mass spectrometry strategy we implemented to fibrillar assemblies remains challenging. Nonetheless, identifying polypeptides originating from molecular chaperones come into close proximity with polypeptide stretches exposed at αSyn fibril surfaces may pave the way for the development of finely targeted ligands that can interfere with αSyn fibril prion-like propagation and subsequent disease progression. Notably, peptides are tunable. Their affinity for their protein targets can be optimized and their pharmacokinetics properties can be adjusted [62].

Author contributions

Conceived the project and designed experiments: EM, VR and RM; performed experiments and analyzed data: MB, VR, LB and TB; provided resources, funding and equipment: RM; wrote the manuscript: MB, and RM.

Acknowledgements

We thank David Cornu for expert assistance in MS and Jeffrey L. Brodsky for the CHIP plasmid. This work was supported by the Centre National de la Recherche Scientifique, the Institut National de la Santé et de la Recherche Médicale, the Région Ile de France through DIM Cerveau et Pensée and the EC Joint Programme on Neurodegenerative Diseases and Agence Nationale pour la Recherche (TransPathND, ANR-17-JPCD-0002-02 and Protest-70, ANR-17-JPCD-0005-01). This work also received support from the EU/EFPIA/Innovative Medicines Initiative 2 Joint Undertaking (IMPRiND grant No. 116060 and PD-MitoQUANT grant No. 821522). This work benefited from the electron microscopy facility Imagerie-Gif and the proteomic facility SICaPS.

Appendix A. Supplementary data

Supplementary data to this article can be found online at https://doi.org/10.1016/j.bbrc.2020.04.091.

References

[1] Spillantini MG, Crowther AR, Jakes R, et al., Filamentous α-synuclein inclusions link multiple system atrophy with Parkinson's disease and dementia with Lewy bodies. Neurosci. Lett. 251 (1998a) 205–208.
[2] Spillantini MG, Crowther AR, Jakes R, et al., Alpha- Synuclein in filamentous inclusions of Lewy bodies from Parkinson's disease and dementia with Lewy bodies. Proc. Natl. Acad. Sci. 95 (1998b) 6469–6473.
[3] P. Brundin, R. Melki, R. Kopito, Prion-like transmission of protein aggregates in neurodegenerative diseases, Nat. Rev. Mol. Cell Biol. 11 (2010) 301–307.
[4] A.A. Davis, C.E.G. Leyns, D.M. Holtzman, Intercellular spread of protein aggregates in neurodegenerative disease, Annu. Rev. Cell Dev. Biol. 34 (2018) 545–568.
[5] P Brundin, R Melki, Prying into the Prion Hypothesis for Parkinson's Disease, J. Neurosci. 37 (2017) 9808–9818.
[6] H. Braak, K. Del Tredici, U. Rüb, et al., Staging of brain pathology related to sporadic Parkinson's disease, Neurobiol. Aging 24 (2003) 197–211.
[7] E Emmanouilidou, K Melachroinou, T Roumeliotis, et al., Cell-Produced a-Synuclein Is Secreted in a Calcium-Dependent Manner by Exosomes and Impacts Neuronal Survival, J. Neurosci. 30 (2010) 6838–6851.
[8] J Ngolab, I Trinh, E Rockenstein, et al., Brain-derived exosomes from dementia with Lewy bodies propagate α-synuclein pathology, Acta Neuropathol. Commun. 5 (2017) 46.
[9] S Abounit, L Bousset, F Loria, et al., Tunneling nanotubes spread fibrillar α-synuclein by intercellular trafficking of lysosomes, EMBO J 35 (2016) 2120–2138.
[10] J Rostami, S Holmqvist, V Lindstrom, et al., Human Astrocytes Transfer Aggregated Alpha-Synuclein via Tunneling Nanotubes, J. Neurosci. 37 (2017) 11835–11853.
[11] M Brahic, L Bousset, G Bieri, et al., Axonal transport and secretion of fibrillar forms of α-synuclein, Aβ42 peptide and HTTExon 1, Acta Neuropathol 131 (2016) 539–548.
[12] P Desplats, H-J Lee, E-J Bae, et al., Inclusion formation and neuronal cell death through neuron-to-neuron transmission of a-synuclein, Proc. Natl. Acad. Sci. 106 (2009) 13010–13015.
[13] H-J Lee, S Patel, S-J Lee, Intravesicular Localization and Exocytosis of a- Synuclein and its Aggregates, J. Neurosci. 25 (2005) 6016–6024.
[14] V. Grozdanov, K.M. Danzer, Release and uptake of pathologic alpha-synuclein, Cell Tissue Res. 373 (2018) 175–182.
[15] L. Rodriguez, M.M. Marano, A. Tandon, Import and export of misfolded α-synuclein, Front. Neurosci. 12 (2018) 1–9.
[16] W.P. Flavin, L. Bousset, Z.C. Green, et al., Endocytic vesicle rupture is a conserved mechanism of cellular invasion by amyloid proteins, Acta Neuropathol. 134 (2017) 629–653.
[17] M. Jucker, L.C. Walker, Self-propagation of pathogenic protein aggregates in neurodegenerative diseases, Nature 501 (2013) 45–51.
[18] W. Peelaerts, L. Bousset, V. Baekelandt, et al., α-Synuclein strains and seeding in Parkinson's disease, incidental Lewy body disease, dementia with Lewy bodies and multiple system atrophy: similarities and differences, Cell Tissue Res. 373 (2018) 195–212.
[19] T. Tyson, J.A. Steiner, P. Brundin, Sorting out release, uptake and processing of alpha-synuclein during prion-like spread of pathology, J. Neurochem. 139 (2016) 275–289.
[20] S. Pemberton, R. Melki, The interaction of Hsc70 protein with fibrillar alpha-Synuclein and its therapeutic potential in Parkinson's disease, Commun. Integr. Biol. 5 (2012) 94–95.
[21] X. Mao, M.T. Ou, S.S. Karuppagounder, et al., Pathological α-synuclein transmission initiated by binding lymphocyte-activation gene 3, Science 353 (2016) aah3374-aah3374.
[22] A.N. Shrivastava, V. Redeker, N. Fritz, et al., α-synuclein assemblies sequester neuronal α3-Na+/K+-ATPase and impair Na+ gradient, EMBO J. 34 (2015) 2408–2423.
[23] A.N. Shrivastava, A. Triller, R. Melki, Cell biology and dynamics of Neuronal Na+/K+-ATPase in health and diseases, Neuropharmacology 169 (2020) 107461, 0–1.
[24] B.E. Stopschinski, B.B. Holmes, G.M. Miller, et al., Specific glycosaminoglycan chain length and sulfation patterns are required for cell uptake of tau versus α-synuclein and β-amyloid aggregates, J. Biol. Chem. 293 (2018) 10826–10840.
[25] AN Shrivastava, A Aperia, R Melki, Triller A Physico-Pathologic Mechanisms Involved in Neurodegeneration: Misfolded Protein-Plasma Membrane Interactions, Neuron 95 (2017) 33–50.
[26] M. Grey, S. Linse, H. Nilsson, et al., Membrane interaction of α-synuclein in different aggregation states, J. Parkinsons Dis. 1 (2011) 359–371.
[27] R.S. Trevino, J.E. Lauckner, Y. Sourigues, et al., Fibrillar structure and charge determine the interaction of polyglutamine protein aggregates with the cell surface, J. Biol. Chem. 287 (2012) 29722–29728.
[28] E.P. De Mattos, A. Wentink, C. Nussbaum-Krammer, C. Hansen, S. Bergink, R. Melki, H.H. Kampinga, Protein quality control pathways at the crossroad of synucleinopathies, J. Parkinsons Dis. 10 (2020) 369–382, https://doi.org/10.3233/JPD-191790.
[29] A. Wentink, C. Nussbaum-Krammer, B. Bukau, Modulation of amyloid states by molecular chaperones, Cold Spring Harb. Perspect. Biol. 11 (2019) a033969.
[30] I.B. Bruinsma, K.A. Bruggink, K. Kinast, et al., Inhibition of α-synuclein aggregation by small heat shock proteins, Protein Struct. Funct. Bioinf. 79 (2011) 2956–2967.
[31] M.M. Dedmon, J. Christodoulou, M.R. Wilson, et al., Heat shock protein 70 inhibits α-synuclein fibril formation via preferential binding to prefibrillar species, J. Biol. Chem. 280 (2005) 14733–14740.
[32] S.F. Falsone, A.J. Kungl, A. Rek, et al., The molecular chaperone Hsp90 modulates intermediate steps of amyloid assembly of the Parkinson-related protein α-synuclein, J. Biol. Chem. 284 (2009) 31190–31199.
[33] S. Pemberton, K. Madiona, L. Pieri, et al., Hsc70 protein interaction with soluble and fibrillar α-synuclein, J. Biol. Chem. 286 (2011) 34690–34699.
[34] A. Rekas, C.G. Adda, J. Andrew Aquilina, et al., Interaction of the molecular chaperone aB-crystallin with a-Synuclein: effects on amyloid fibril formation and chaperone activity, J. Mol. Biol. 340 (2004) 1167–1183.
[35] C. Roodveldt, C.W. Bertoncini, A. Andersson, et al., Chaperone proteostasis in Parkinson's disease: stabilization of the hsp70/α-synuclein complex by hip, EMBO J. 28 (2009) 3758–3770.
[36] F.A. Aprile, P. Arosio, G. Fusco, et al., Inhibition of α-synuclein fibril elongation by Hsp70 is governed by a kinetic binding competition between α-synuclein species, Biochemistry 56 (2017) 1177–1180.
[37] D. Cox, E. Selig, M.D.W. Griffin, et al., Small Heat-shock Proteins Prevent α-synuclein aggregation via transient interactions and their efficacy is affected by the rate of aggregation, J. Biol. Chem. 291 (2016) 22618–22629.
[38] X. Gao, M. Carroni, C. Nussbaum-Krammer, et al., Human Hsp70 disaggregase reverses Parkinson's-linked α-synuclein amyloid fibrils, Moo. Cell. 59 (2015) 781–793.
[39] C. Nury, V. Redeker, S. Dautrey, et al., A novel bio-orthogonal cross-linker for improved protein/protein interaction analysis, Anal. Chem. 87 (2015)

1853–1860.
[40] V. Redeker, S. Pemberton, W. Bienvenut, et al., Identification of protein interfaces between α-synuclein, the principal component of Lewy bodies in Parkinson disease, and the molecular chaperones human Hsc70 and the yeast Ssa1p, J. Biol. Chem. 287 (2012) 32630–32639.
[41] C.A. Waudby, T.P.J. Knowles, G.L. Devlin, et al., The interaction of αB-crystallin with mature α-synuclein amyloid fibrils inhibits their elongation, Biophys. J. 98 (2010) 843–851.
[42] JA Aquilina, JLP Benesch, OA Bateman, et al., Polydispersity of a mammalian chaperone: Mass spectrometry reveals the population of oligomers in B-crystallin, Proc. Natl. Acad. Sci. 100 (2003) 10611–10616.
[43] H. Braak, K. Del Tredici, D. Sandmann-Keil, et al., Nerve cells expressing heat-shock proteins in Parkinson's disease, Acta Neuropathol. 102 (2001) 449–454.
[44] A. Mainz, J. Peschek, M. Stavropoulou, et al., The chaperone αB-crystallin uses different interfaces to capture an amorphous and an amyloid client, Nat. Struct. Mol. Biol. 22 (2015) 898–905.
[45] M. Zhang, M. Windheim, S.M. Roe, et al., Chaperoned ubiquitylation—crystal structures of the CHIP U box E3 ubiquitin ligase and a CHIP-Ubc13-Uev1a complex, Mol. Cell. 20 (2005) 525–538.
[46] Y. Shin, J. Klucken, C. Patterson, et al., The Co-chaperone carboxyl terminus of Hsp70-interacting protein (CHIP) mediates a-synuclein degradation decisions between proteasomal and lysosomal pathways, J. Biol. Chem. 280 (2005) 23727–23734.
[47] J.E. Tetzlaff, P. Putcha, T.F. Outeiro, et al., CHIP targets toxic α-synuclein oligomers for degradation, J. Biol. Chem. 283 (2008) 17962–17968.
[48] M. Ghee, R. Melki, N. Michot, et al., PA700, the regulatory complex of the 26S proteasome, interferes with α-synuclein assembly, FEBS J. 272 (2005) 4023–4033.
[49] A. Shevchenko, M. Wilm, O. Vorm, et al., Mass spectrometric sequencing of proteins from silver-stained polyacrylamide gels, Anal. Chem. 68 (1996) 850–858.
[50] A.N. Shrivastava, V. Redeker, L. Pieri, et al., Clustering of Tau fibrils impairs the synaptic composition of α3-Na +/K + -ATPase and AMPA receptors, EMBO J. 38 (2019), e99871.
[51] M. Götze, J. Pettelkau, S. Schaks, et al., StavroX-A software for analyzing crosslinked products in protein interaction studies, J. Am. Soc. Mass Spectrom. 23 (2012) 76–87.
[52] I. Migneault, C. Dartiguenave, M.J. Bertrand, et al., Glutaraldehyde: behavior in aqueous solution, reaction with proteins, and application to enzyme cross-linking, Biotechniques 37 (2004) 790–802.
[53] C. Hansen, E. Angot, A. Bergström, et al., α-Synuclein propagates from mouse brain to grafted dopaminergic neurons and seeds aggregation in cultured human cells, J. Clin. Invest. 121 (2011) 715–725.
[54] E. Monsellier, V. Redeker, G. Ruiz-Arlandis, et al., Molecular interaction between the chaperone Hsc70 and the N-terminal flank of huntingtin exon 1 modulates aggregation, J. Biol. Chem. 290 (2015) 2560–2576.
[55] V. Redeker, J. Bonnefoy, J.P. Le Caer, et al., A region within the C-terminal domain of Ure2p is shown to interact with the molecular chaperone Ssa1p by the use of cross-linkers and mass spectrometry, FEBS J. 277 (2010) 5112–5123.
[56] R. Guerrero-Ferreira, N.M.I. Taylor, A.-A. Arteni, et al., Two new polymorphic structures of alpha-synuclein solved by cryo-electron microscopy, Elife 8 (2019) pii:e48907, https://doi.org/10.7554/eLife.48907.
[57] H Dimant, D Ebrahimi-Fakhari, McLean PJMolecular chaperones and cochaperones in parkinson disease, Neuroscientist 18 (2012) 589–601.
[58] I Lindberg, J Shorter, RL Wiseman, et al., Chaperones in Neurodegeneration, J. Neurosci. 35 (2015) 13853–13859.
[59] Z Liu, C Wang, Y Li, et al., Mechanistic insights into the switch of αB-crystallin chaperone activity and self-multimerization, J. Biol. Chem. 293 (2018) 14880–14890.
[60] GK a Hochberg, H. Ecroyd, C. Liu, et al., The structured core domain of αB-crystallin can prevent amyloid fibrillation and associated toxicity, Proc. Natl. Acad. Sci. U. S. A. 111 (2014) 200–203.
[61] D. Cox, D.R. Whiten, J.W.P. Brown, et al., The small heat shock protein Hsp27 binds α-synuclein fibrils, preventing elongation and cytotoxicity, J. Biol. Chem. 293 (2018) 4486–4497.
[62] L. Di, Strategic approaches to optimizing peptide ADME properties, AAPS J. 17 (2015) 134–143.

Please cite this article as: M. Bendifallah et al., Interaction of the chaperones alpha B-crystallin and CHIP with fibrillar alpha-synuclein: Effects on internalization by cells and identification of interacting interfaces, Biochemical and Biophysical Research Communications, https://doi.org/10.1016/j.bbrc.2020.04.091